

Modification of the halo mass function by kurtosis associated with primordial non-Gaussianity

Shuichiro Yokoyama¹, Naoshi Sugiyama^{1,2}, Saleem Zaroubi^{3,4} and Joseph Silk⁵

¹ Department of Physics and Astrophysics, Nagoya University, Aichi 464-8602, Japan

² Institute for the Physics and Mathematics of the Universe, University of Tokyo, Kashiwa, Chiba, 277-8568, Japan

³ Kapteyn Astronomical Institute, University of Groningen, P.O. Box 800, 9700 AV Groningen, the Netherlands

⁴ Physics Department, Technion, Haifa 32000, Israel

⁵ Oxford University, Astrophysics, Denys Wilkinson Building, Keble Road, Oxford, OX1, 3RH, UK

24 February 2024

ABSTRACT

We study the halo mass function in the presence of a kurtosis type of primordial non-Gaussianity. The kurtosis corresponds to the trispectrum as defined in Fourier space. The primordial trispectrum is commonly characterized by two parameters, τ_{NL} and g_{NL} . We focus on τ_{NL} which is an important parameter to test the physics of multi-field inflation models. As applications of the derived non-Gaussian mass function, we consider the effects on the abundance of void structure, on early star formation, and on formation of the most massive objects at high redshift. We show that by comparing the effects of primordial non-Gaussianity on cluster abundance with that on void abundance, we can distinguish between the skewness and the kurtosis types of primordial non-Gaussianity. As for early star formation, we show that the kurtosis type of primordial non-Gaussianity seems on the average not to affect the reionization history of the Universe. However, at high redshifts (up to $z \simeq 20$) such non-Gaussianity does somewhat affect the early stages of reionization.

Key words: :Inflation, large scale structure of the Universe

1 INTRODUCTION

The inflation paradigm has been well-known as a successful scenario for resolving several shortcomings of the standard Big Bang Model, in particular, the generation of primordial fluctuations which seed cosmic microwave background (CMB) fluctuations and structure formation of the Universe. In the standard inflationary scenario, the primordial density fluctuations are generated from quantum fluctuations of a scalar field and they have almost Gaussian statistics. In recent years it has been realized that studying the non-Gaussianity of the primordial density fluctuations can reveal valuable information about the dynamics of inflation (Komatsu & Spergel 2001; Bartolo et al. 2004; Bartolo, Matarrese & Riotto 2010; Komatsu 2010) (and references therein). Thanks to significant progress in cosmological observations, most notably the CMB observations, we may expect that a meaningful measurement of this quantity will become observationally available in the near future and will thereby allow several inflation models to be tested.

In Ref. (Komatsu & Spergel 2001), the authors have introduced a simple new parameter which describes the deviation from Gaussianity of the statistics of the primordial curvature fluctuations, the so-called non-linearity parameter f_{NL} , defined as (Salopek & Bond 1990; Gangui et al. 1994; Verde et al. 2000)

$$\zeta(\mathbf{x}) = \zeta_{\text{G}}(\mathbf{x}) + \frac{3}{5}f_{\text{NL}}(\zeta_{\text{G}}^2(\mathbf{x}) - \langle \zeta_{\text{G}}(\mathbf{x})^2 \rangle) + O(\zeta_{\text{G}}^3(\mathbf{x})), \quad (1)$$

where ζ represents the primordial curvature fluctuations on a uniform energy density hypersurface and ζ_{G} denotes the Gaussian part. In the Probability Density Function (PDF) of the primordial fluctuations, the non-zero value of the non-linearity parameter f_{NL} may generate a non-zero value of the skewness (3rd order moment), the kurtosis (4-th order moment) and so on. Obviously, the skewness can be parametrized by the leading term using f_{NL} . However, the kurtosis can be affected not only by the f_{NL} term but also by higher order terms, such as the $\zeta_{\text{G}}^3(\mathbf{x})$ term in the above expression (1). In general, one needs two parameters in order to characterize the kurtosis in the PDF. These parameters are normally called τ_{NL} and g_{NL} , where the first is usually (although not always) related to f_{NL} and the second is the parameter that characterizes the third moment of ζ . Such kind of non-linearity is the so-called local type of non-Gaussianity. Recently, other types of non-Gaussianity have been discussed in the literature, *e.g.*, equilateral and orthogonal types. Theoretically, the local type of non-Gaussianity can be generated from the super-horizon non-linear dynamics of primordial curvature perturbations. On the other hand, the equilateral and orthogonal types of non-Gaussianity can be generated when one considers a scalar field which has a non-canonical kinetic term or the higher order derivative correction terms. In this paper, we focus on the local type of non-Gaussianity and consider the case where the equilateral and orthogonal types are negligible.

In the case where the primordial curvature fluctuations were generated from single field stochastic fluctuations (single-sourced case), *i.e.*, the primordial curvature fluctuations can be expressed as Eq. (1), and τ_{NL} can be described only by f_{NL} . But in general, *e.g.*, if the primordial curvature fluctuations were generated from multi-stochastic fluctuations then τ_{NL} and f_{NL} have no universal relation any more (Suyama & Yamaguchi 2008; Suyama et al. 2010; Sugiyama, Komatsu & Futamase 2011). Hence, it seems to be important to investigate the observational consequences of τ_{NL} independently of f_{NL} .

In this paper, we focus on the effects of the kurtosis type of primordial non-Gaussianity on the Large Scale Structure (LSS), in particular, on the halo mass function. There are many studies of the effects of primordial non-Gaussianity on the LSS and also on the formulation of the non-Gaussian halo mass function (Matarrese, Verde & Jimenez 2000; Slosar et al. 2008; Maggiore & Riotto 2010; Verde 2010; D’Amico et al. 2010; De Simone, Maggiore & Riotto 2010; Wagner, Verde & Boubekeur 2010) (and references therein), which focus not only on f_{NL} -type but also g_{NL} -type (Desjacques & Seljak 2010; Maggiore & Riotto 2010; Chongchitnan & Silk 2010a,b; Enqvist, Hotchkiss & Taanila 2010). Here, we study the effects of kurtosis of the non-Gaussian primordial fluctuations whose non-linearity is parameterized by the two free parameters, g_{NL} and τ_{NL} . Recently, a number of authors have studied non-Gaussian initial perturbations in two-field inflationary models (Tseliakhovich, Hirata & Slosar 2010; Smith & LoVerde 2010). In these papers, the authors have considered the effect of non-Gaussianity on the halo bias. Although this type of primordial non-Gaussianity is similar to the one considered here, we study the effects on the halo mass function.

This paper is organized as follows. In the next section, we briefly review the kurtosis type of primordial non-Gaussianity considered here. In section 3, we formulate halo mass functions with primordial non-Gaussianity, based on the Press-Schechter theory and Edgeworth expansion. In section 4, we apply the non-Gaussian halo mass function to the formation of astrophysical objects. We consider three applications: early star formation, the most massive object at high redshift and the abundance of voids. Section 5 provides a discussion and summary of our results. We adopt throughout the best fit cosmological parameters taken from WMAP 7-year data.

2 TRISPECTRUM OF PRIMORDIAL NON-GAUSSIAN CURVATURE FLUCTUATIONS

Here, we focus on the local-type non-Gaussianity. Following the notation commonly used, in the single-sourced case, up to the third order, the primordial curvature fluctuations can be expressed as

$$\zeta = \zeta_G + \frac{3}{5}f_{\text{NL}}(\zeta_G^2 - \langle \zeta_G^2 \rangle) + \frac{9}{25}g_{\text{NL}}\zeta_G^3. \quad (2)$$

Based on this expression, the trispectrum of ζ is given by

$$\begin{aligned} \langle \zeta(\mathbf{k}_1)\zeta(\mathbf{k}_2)\zeta(\mathbf{k}_3)\zeta(\mathbf{k}_4) \rangle &= (2\pi)^3 T_\zeta(k_1, k_2, k_3, k_4) \delta^{(3)}(\mathbf{k}_1 + \mathbf{k}_2 + \mathbf{k}_3 + \mathbf{k}_4), \\ T_\zeta(k_1, k_2, k_3, k_4) &= \tau_{\text{NL}}(P_\zeta(k_1)P_\zeta(k_2)P_\zeta(k_{13}) + 11\text{perms.}) + \frac{54}{25}g_{\text{NL}}(P_\zeta(k_1)P_\zeta(k_2)P_\zeta(k_3) + 3\text{perms.}), \end{aligned} \quad (3)$$

where $k_{13} = |\mathbf{k}_1 + \mathbf{k}_3|$ and $P_\zeta(k_1)$ is a power spectrum of ζ given by $\langle \zeta(\mathbf{k}_1)\zeta(\mathbf{k}_2) \rangle = (2\pi)^3 P(k_1) \delta^{(3)}(\mathbf{k}_1 + \mathbf{k}_2)$. For the above definition of τ_{NL} and the form of the non-linearity of the curvature perturbation (2), τ_{NL} can be written in terms of the non-linearity parameter f_{NL} as

$$\tau_{\text{NL}} = \frac{36}{25}f_{\text{NL}}^2. \quad (4)$$

This consistency relation is satisfied only in the case where the primordial curvature fluctuations can be described by Eq. (2), namely, the primordial curvature fluctuations are sourced only from the quantum fluctuations of a single scalar field, *e.g.*, curvaton (Enqvist & Sloth 2002; Lyth & Wands 2002; Moroi & Takahashi 2001).

However, if there are multiple sources of the primordial curvature fluctuations, then the above consistency relation is not satisfied (Langlois & Vernizzi 2004; Ichikawa et al. 2008; Huang 2009; Byrnes & Choi 2010). In general, it has been known that there exists an inequality between the local type non-linearity parameters τ_{NL} and f_{NL} given by (Suyama & Yamaguchi 2008; Suyama et al. 2010; Sugiyama, Komatsu & Futamase 2011)

$$\tau_{\text{NL}} > \frac{1}{2} \left(\frac{6}{5}f_{\text{NL}} \right)^2. \quad (5)$$

For example, let us consider the local-type non-Gaussianity given by

$$\zeta = \phi_G + \frac{3}{5}f_{\text{NL}}(\phi_G^2 - \langle \phi_G^2 \rangle) + t_{\text{NL}}\phi_G\psi_G, \quad (6)$$

where ϕ_G and ψ_G are Gaussian fluctuations with $\langle \phi_G\psi_G \rangle = 0$ and t_{NL} is a non-linearity parameter, which represents the non-linear coupling between ϕ_G and ψ_G in ζ_G . At leading order, the power spectrum of ζ is given by that of the Gaussian part ϕ_G as

$$\langle \zeta(\mathbf{k})\zeta(\mathbf{k}') \rangle = \langle \phi_G(\mathbf{k})\phi_G(\mathbf{k}') \rangle = (2\pi)^3 P_\phi(k) \delta^{(3)}(\mathbf{k} + \mathbf{k}'), \quad (7)$$

and the bispectrum is given only by f_{NL} as

$$\langle \zeta(\mathbf{k}_1)\zeta(\mathbf{k}_2)\zeta(\mathbf{k}_3) \rangle = (2\pi)^3 \frac{6}{5}f_{\text{NL}}(P_\phi(k_1)P_\phi(k_2) + 2\text{perms.}) \delta^{(3)}(\mathbf{k}_1 + \mathbf{k}_2 + \mathbf{k}_3), \quad (8)$$

because of $\langle \phi_G\psi_G \rangle = 0$.

In the single-source case which corresponds to the case of $t_{\text{NL}} = 0$, as mentioned above, the trispectrum can be also parameterized only by f_{NL} . However, for the above type of curvature fluctuations the trispectrum is given by

$$\begin{aligned}
 T_\zeta(k_1, k_2, k_3, k_4) = & \left(\frac{6}{5}f_{\text{NL}}\right)^2 (P_\phi(k_1)P_\phi(k_2)P_\phi(k_{13}) + 11\text{perms.}) \\
 & + t_{\text{NL}}^2 \left(P_\phi(k_1)P_\phi(k_2)P_\psi(k_{13}) + P_\phi(k_1)P_\phi(k_2)P_\psi(k_{14}) + P_\phi(k_1)P_\phi(k_3)P_\psi(k_{12}) \right. \\
 & \quad + P_\phi(k_1)P_\phi(k_3)P_\psi(k_{14}) + P_\phi(k_1)P_\phi(k_4)P_\psi(k_{12}) + P_\phi(k_1)P_\phi(k_4)P_\psi(k_{13}) \\
 & \quad + P_\phi(k_2)P_\phi(k_3)P_\psi(k_{12}) + P_\phi(k_2)P_\phi(k_3)P_\psi(k_{24}) + P_\phi(k_2)P_\phi(k_4)P_\psi(k_{12}) \\
 & \quad \left. + P_\phi(k_2)P_\phi(k_4)P_\psi(k_{23}) + P_\phi(k_3)P_\phi(k_4)P_\psi(k_{13}) + P_\phi(k_3)P_\phi(k_4)P_\psi(k_{23}) \right), \tag{9}
 \end{aligned}$$

where $k_{13} = |\mathbf{k}_1 + \mathbf{k}_3|$. We assume that the power spectra of random Gaussian fields ϕ_G and ψ_G have only weak scale-dependence, that is, the power spectra are respectively given by

$$P_\phi(k) \equiv \frac{2\pi^2}{k^3} A_\phi \left(\frac{k}{k_0}\right)^{n_\phi - 1}, \quad P_\psi(k) \equiv \frac{2\pi^2}{k^3} A_\psi \left(\frac{k}{k_0}\right)^{n_\psi - 1}, \tag{10}$$

where k_0 is a pivot scale and $|n_\phi - 1| \ll 1$ and $|n_\psi - 1| \ll 1$. In such a case, we can rewrite the power spectrum of ψ_G as

$$P_\psi(k) \simeq \alpha P_\phi(k), \quad \alpha \equiv A_\psi/A_\phi, \tag{11}$$

and then using the ratio of the amplitudes α , the expression for the trispectrum can be reduced to

$$\langle \zeta(\mathbf{k}_1)\zeta(\mathbf{k}_2)\zeta(\mathbf{k}_3)\zeta(\mathbf{k}_4) \rangle \simeq (2\pi)^3 \delta^{(3)}(\mathbf{k}_1 + \mathbf{k}_2 + \mathbf{k}_3 + \mathbf{k}_4) \left(\frac{36}{25}f_{\text{NL}}^2 + \alpha t_{\text{NL}}^2\right) (P_\phi(k_1)P_\phi(k_2)P_\phi(k_{13}) + 11\text{perms.}). \tag{12}$$

From the above equation and Eq. (3), we easily find that the non-linearity parameter τ_{NL} is

$$\tau_{\text{NL}} = \frac{36}{25}f_{\text{NL}}^2 + \alpha t_{\text{NL}}^2 \geq \frac{36}{25}f_{\text{NL}}^2. \tag{13}$$

Hence, in the following discussion, we consider τ_{NL} independently of f_{NL} .

3 NON-GAUSSIAN MASS FUNCTION INDUCED FROM PRIMORDIAL NON-GAUSSIANITY

In the previous section, we have shown that there is a strong theoretical motivation for considering τ_{NL} to be independent of f_{NL} . The parameter τ_{NL} characterizes the amplitude of the trispectrum of primordial curvature fluctuations as well as g_{NL} . Here, we briefly review the formula for the halo mass function with not only the non-zero primordial bispectrum but also the non-zero primordial trispectrum, based on Press-Schechter theory.

3.1 Probability Density Function of the smoothed density field with primordial non-Gaussianity

The matter density linear fluctuations in Fourier space at redshift z , $\delta(\mathbf{k}, z)$, are given by the primordial curvature perturbation on a uniform energy density hypersurface $\zeta(\mathbf{k})$ as

$$\delta(\mathbf{k}, z) = \mathcal{M}(k)D(z)\zeta(\mathbf{k}), \tag{14}$$

$$\mathcal{M}(k) = \frac{2}{5} \frac{1}{\Omega_{m0}} \frac{k^2}{H_0^2} T(k), \tag{15}$$

where Ω_{m0} is the present density parameter for total non-relativistic matter, H_0 is the Hubble constant, $D(z)$ is a linear growth function and $T(k)$ is a transfer function. Using these expressions, we can obtain the linear matter power spectrum as

$$\langle \delta(\mathbf{k}, z)\delta(\mathbf{k}', z) \rangle \equiv (2\pi)^3 P_\delta(k, z)\delta^{(3)}(\mathbf{k} + \mathbf{k}'), \tag{16}$$

$$P_\delta(k, z) = \frac{2\pi^2}{k^3} \mathcal{M}(k)^2 D(z)^2 \mathcal{P}_\phi(k), \tag{17}$$

where $\mathcal{P}_\phi(k) = k^3 P_\phi(k)/(2\pi^2)$. Following the standard procedure, let us define the smoothed density fluctuation on a given length scale, R , as

$$\delta_R = \int \frac{d^3\mathbf{k}}{(2\pi)^3} W_R(k)\delta(\mathbf{k}, z), \tag{18}$$

where $W_R(k)$ is the Fourier transform of a spherical top-hat window function given by

$$W_R(k) = 3 \left(\frac{\sin(kR)}{k^3 R^3} - \frac{\cos(kR)}{k^2 R^2} \right). \quad (19)$$

In order to take into account primordial non-Gaussianity in the smoothed density fluctuations, let us consider the PDF of δ_R , $F(\delta_R)d\delta_R$. The n -th central moment for $F(\delta_R)d\delta_R$ is defined as

$$\langle \delta_R^n \rangle \equiv \int_{-\infty}^{\infty} \delta_R^n F(\delta_R) d\delta_R, \quad (20)$$

and each reduced p -th cumulant can be defined as

$$S_p(R) \equiv \frac{\langle \delta_R^p \rangle_c}{\langle \delta_R^2 \rangle_c^{p/2}}, \quad (21)$$

where a subscript c denotes the connected part of p -point function given by

$$\begin{aligned} \langle \delta_R \rangle_c &= 0, \quad \langle \delta_R^2 \rangle_c = \langle \delta_R^2 \rangle \equiv \sigma_R^2, \\ \langle \delta_R^3 \rangle_c &= \langle \delta_R^3 \rangle, \quad \langle \delta_R^4 \rangle_c = \langle \delta_R^4 \rangle - 3\langle \delta_R^2 \rangle_c^2, \text{ etc.}, \end{aligned} \quad (22)$$

with zero mean density field. Here, σ_R^2 , $S_3(R)$ and $S_4(R)$ are the variance, the skewness and the kurtosis, respectively. Let us consider a non-Gaussian PDF of matter density fluctuations, based on the concept of the Edgeworth expansion. Here, we consider the expansion of the PDF of the density field $F(\nu)d\nu$ with $\nu \equiv \delta_R/\sigma_R$ in terms of the derivatives of the Gaussian PDF, $F_G(\nu)$, as (Juszkiewicz et al. 1995; LoVerde et al. 2008)

$$F(\nu)d\nu = d\nu \left[c_0 F_G(\nu) + \sum_{m=1}^{\infty} \frac{c_m}{m!} F_G^{(m)}(\nu) \right], \quad (23)$$

with

$$F_G(\nu) \equiv (2\pi)^{-1/2} \exp(-\nu^2/2), \quad (24)$$

$$F_G^{(m)}(\nu) \equiv \frac{d^m}{d\nu^m} F_G(\nu) = (-1)^m H_m(\nu) F_G(\nu), \quad (25)$$

where $H_m(\nu)$ is the Hermite polynomials;

$$\begin{aligned} H_1(\nu) &= \nu, \quad H_2(\nu) = \nu^2 - 1, \quad H_3(\nu) = \nu^3 - 3\nu, \\ H_4(\nu) &= \nu^4 - 6\nu^2 + 3, \quad H_5(\nu) = \nu^5 - 10\nu^3 + 15\nu, \dots \end{aligned} \quad (26)$$

From the above relation between the derivatives of the Gaussian PDF and Hermite polynomials, we can regard the expression (23) as a non-Gaussian PDF expanded in terms of the Hermite polynomials. Since the Hermite polynomials satisfy orthogonal relations;

$$\int_{-\infty}^{\infty} H_m(\nu) H_n(\nu) F_G(\nu) d\nu = \begin{cases} 0 & , \text{ if } m \neq n, \\ m! & , \text{ if } m = n, \end{cases} \quad (27)$$

we can evaluate the coefficients as

$$c_m = (-1)^m \int_{-\infty}^{\infty} H_m(\nu) F(\nu) d\nu. \quad (28)$$

Then, we can obtain the expressions for the coefficients, c_m , in terms of the reduced cumulants (variance, skewness, kurtosis and so on) as

$$\begin{aligned} c_0 &= 1, \quad c_1 = c_2 = 0, \quad c_3 = -S_3(R)\sigma_R, \quad c_4 = S_4(R)\sigma_R^2, \\ c_5 &= -S_5(R)\sigma_R^3, \quad c_6 = 10S_3(R)^2\sigma_R^2 + S_6(R)\sigma_R^4, \dots \end{aligned} \quad (29)$$

and, as a result, the non-Gaussian PDF of the density field, $F(\nu)d\nu$, can be obtained as

$$\begin{aligned} F(\nu)d\nu &= \frac{d\nu}{\sqrt{2\pi}} \exp(-\nu^2/2) \left[1 + \frac{S_3(R)\sigma_R}{6} H_3(\nu) + \frac{1}{2} \left(\frac{S_3(R)\sigma_R}{6} \right)^2 H_6(\nu) + \frac{1}{6} \left(\frac{S_3(R)\sigma_R}{6} \right)^3 H_9(\nu) \right. \\ &\quad \left. + \frac{S_4(R)\sigma_R^2}{24} H_4(\nu) + \frac{1}{2} \left(\frac{S_4(R)\sigma_R^2}{24} \right)^2 H_8(\nu) + \frac{1}{6} \left(\frac{S_4(R)\sigma_R^2}{24} \right)^3 H_{12}(\nu) + \dots \right], \end{aligned} \quad (30)$$

up to the third order terms in $S_3(R)$ and $S_4(R)$ and neglect the contributions of the higher order cumulants; $S_n(R)$ ($n \geq 5$). This derivation of the non-Gaussian PDF is based on the so-called Edgeworth expansion. Of course, the non-zero non-linearity parameters f_{NL} , τ_{NL} and g_{NL} also generate non-zero higher order cumulants; $S_n(R)$ ($n \geq 5$). However, as far as considering the non-Gaussian curvature fluctuations given by Eq. (6) and current observational constraints on the non-linearity parameters (Komatsu et al. 2011; Fergusson, Regan & Shellard 2010), terms $S_n(R)$ ($n \geq 5$) are greatly suppressed (Enqvist, Hotchkiss & Taanila 2010). Hence, the assumption of neglecting the higher order cumulants seems to be reasonable.

3.2 Halo mass function with non-Gaussian corrections

Let us consider the halo mass function with non-Gaussian PDF of the smoothed density field as given in the previous subsection. Based on the spirit of the Press-Schechter formula, the halo mass function which gives the number density of collapsed structures (halos) with the mass between $M(= 4\pi\bar{\rho}R^3/3$ with $\bar{\rho}$ is the background matter density) and $M + dM$ at a redshift z , $(dn(M, z)/dM)dM$ is given by (D'Amico et al. 2010)

$$\begin{aligned} \frac{dn}{dM}(M, z)dM &= -dM \frac{2\bar{\rho}}{M} \frac{d}{dM} \int_{\delta_c/\sigma_R}^{\infty} d\nu F(\nu) \\ &= -dM \sqrt{\frac{2}{\pi}} \frac{\bar{\rho}}{M} \exp\left[-\frac{\nu_c^2}{2}\right] \left\{ \frac{d \ln \sigma_R}{dM} \nu_c \left[1 \right. \right. \\ &\quad \left. \left. + \frac{S_3(R)\sigma_R}{6} H_3(\nu_c) + \frac{1}{2} \left(\frac{S_3(R)\sigma_R}{6} \right)^2 H_6(\nu_c) + \frac{1}{6} \left(\frac{S_3(R)\sigma_R}{6} \right)^3 H_9(\nu_c) \right. \right. \\ &\quad \left. \left. + \frac{S_4(R)\sigma_R^2}{24} H_4(\nu_c) + \frac{1}{2} \left(\frac{S_4(R)\sigma_R^2}{24} \right)^2 H_8(\nu_c) + \frac{1}{6} \left(\frac{S_4(R)\sigma_R^2}{24} \right)^3 H_{12}(\nu_c) \right] \right. \\ &\quad \left. + \frac{d}{dM} \left(\frac{S_3(R)\sigma_R}{6} \right) H_2(\nu_c) + \frac{1}{2} \frac{d}{dM} \left(\frac{S_3(R)\sigma_R}{6} \right)^2 H_5(\nu_c) + \frac{1}{6} \frac{d}{dM} \left(\frac{S_3(R)\sigma_R}{6} \right)^3 H_8(\nu_c) \right. \\ &\quad \left. + \frac{d}{dM} \left(\frac{S_4(R)\sigma_R^2}{24} \right) H_3(\nu_c) + \frac{1}{2} \frac{d}{dM} \left(\frac{S_4(R)\sigma_R^2}{24} \right)^2 H_7(\nu_c) + \frac{1}{6} \frac{d}{dM} \left(\frac{S_4(R)\sigma_R^2}{24} \right)^3 H_{11}(\nu_c) \right\} + \dots \quad (31) \end{aligned}$$

where $\nu_c = \delta_c/\sigma_R$ and δ_c denotes the threshold for collapse which is originally given by $\delta_c \approx 1.69$. However, in Ref. (Grossi et al. 2009), the authors have suggested that using the correction $\delta_c \rightarrow \delta_c \sqrt{q}$ with $q = 0.75$ puts the analytic predictions in good agreement with the numerical simulations. This is due to the more realistic case of ellipsoidal collapse. Hence $\delta_c = 1.69 \times \sqrt{q}$ is often referred to as the critical density of ellipsoidal collapse. Here we adopt this corrected density threshold $\delta_c = 1.69 \times \sqrt{0.75}$. In the following calculations, we use the above formula of the non-Gaussian mass functions up to the third order in terms of S_3 and S_4 .

For a Gaussian probability distribution, the mass function is given by

$$\frac{dn_G}{dM}(M, z)dM = -\sqrt{\frac{2}{\pi}} \frac{\bar{\rho}}{M} \exp\left[-\frac{\nu_c^2}{2}\right] \frac{d \ln \sigma_R}{dM} \nu_c dM, \quad (32)$$

and we define the ratio between the non-Gaussian mass function and the Gaussian one as¹

$$\mathcal{R}_{\text{NG}}(M, z) \equiv \frac{dn(M, z)/dM}{dn_G(M, z)/dM}. \quad (34)$$

Let us focus on the redshift dependence of the above expression. From the definition of the reduced cumulants (21) and the fact that the redshift dependence of the density field is given by $\delta_R \propto D(z)$, we can easily find that $\sigma^{p-2} S_p(R)$ has no redshift-dependence. Hence, any remaining redshift dependence comes only from the term $\frac{\delta_c}{\sigma_R}$. Here, following the literature, the redshift-dependence can be carried by δ_c as $\delta_c \rightarrow \delta_c(z) \propto D(z)^{-1}$ and then the variance σ_R has no redshift-dependence. In the following discussion, we change the subscript R to M because R and M have a one-to-one correspondence through the equation $M = 4\pi R^3 \bar{\rho}/3$.

3.2.1 Variance, skewness and kurtosis

Let us consider the concrete expressions of the variance, skewness and kurtosis of the primordial curvature perturbations whose power-, bi- and tri-spectra are given by Eqs. (7), (8) and (3), respectively. The variance is given by

$$\sigma_R^2 = \int \frac{dk}{k} W_R^2(k) \mathcal{M}(k)^2 \mathcal{P}_\phi(k), \quad (35)$$

¹ In Refs. (Enqvist, Hotchkiss & Taanila 2010; Matarrese, Verde & Jimenez 2000; Verde et al. 2001), the authors introduced the MVJ convention for defining the ratio given by

$$\begin{aligned} \mathcal{R}_{\text{NG}}^{\text{MVJ}}(\mathcal{M}, \ddagger) &= \exp \left[\nu_c^3 \frac{S_3(R)\sigma_R}{6} + \nu_c^4 \frac{S_4(R)\sigma_R^2}{24} \right] \times \left[\delta_3 + \frac{\nu_c}{\delta_3} \left(-\frac{S_3(R)\sigma_R}{6} \right) + \left(\frac{d \ln \sigma_R}{dM} \right)^{-1} \frac{d}{dM} \left(\frac{S_3(R)\sigma_R}{6} \right) \right] \\ &\quad \times \left[\delta_4 + \frac{\nu_c^2}{\delta_4} \left(-\frac{S_4(R)\sigma_R^2}{12} \right) + \left(\frac{d \ln \sigma_R}{dM} \right)^{-1} \frac{d}{dM} \left(\frac{S_4(R)\sigma_R^2}{24} \right) \right], \\ \delta_3 &\equiv \left(1 - \nu_c \frac{S_3(R)\sigma_R}{3} \right)^{1/2}, \quad \delta_4 \equiv \left(1 - \nu_c^2 \frac{S_4(R)\sigma_R^2}{12} \right)^{1/2}, \end{aligned} \quad (33)$$

which is not based on the Edgeworth expansion. In our calculation, we have also checked the consistency between the above MVJ expression and Eq. (34). This issue is discussed in Appendix A.

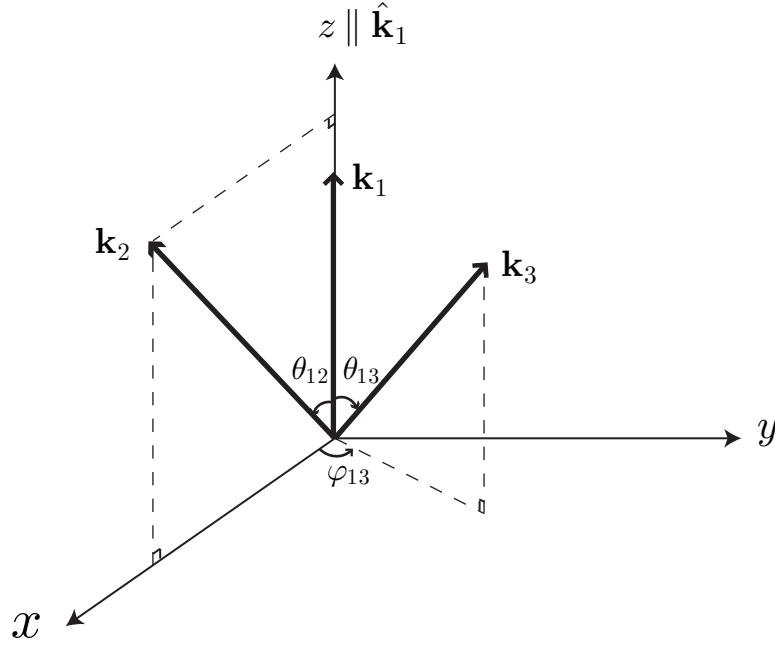


Figure 1. the three vectors, \mathbf{k}_1 , \mathbf{k}_2 and \mathbf{k}_3 in the trispectrum.

the skewness is (Chongchitnan & Silk 2010a)

$$\begin{aligned}
 S_3(R) &\equiv \frac{6}{5} \frac{f_{\text{NL}}}{\sigma_R^4} \tilde{S}_3(R), \\
 \tilde{S}_3(R) &= \int \frac{dk_1}{k_1} W_R(k_1) \mathcal{M}(k_1) \mathcal{P}_\phi(k_1) \int \frac{dk_2}{k_2} W_R(k_2) \mathcal{M}(k_2) \mathcal{P}_\phi(k_2) \\
 &\quad \times \int \frac{d\mu_{12}}{2} W_R(k_{12}) \mathcal{M}(k_{12}) \left[1 + \frac{P_\phi(k_{12})}{P_\phi(k_1)} + \frac{P_\phi(k_{12})}{P_\phi(k_2)} \right], \tag{36}
 \end{aligned}$$

where $k_{12} = \sqrt{k_1^2 + k_2^2 + 2k_1k_2\mu_{12}}$ and $\mu_{12} = \cos \theta_{12}$, and the kurtosis which is proportional to the non-linearity parameter τ_{NL} is given by

$$\begin{aligned}
 S_4^\tau(R) &\equiv \frac{\tau_{\text{NL}}}{\sigma_R^6} \tilde{S}_4^\tau(R), \\
 \tilde{S}_4^\tau(R) &= \int \frac{dk_1}{k_1} W_R(k_1) \mathcal{M}(k_1) \mathcal{P}_\phi(k_1) \int \frac{dk_2}{k_2} W_R(k_2) \mathcal{M}(k_2) \mathcal{P}_\phi(k_2) \int \frac{dk_3}{k_3} W_R(k_3) \mathcal{M}(k_3) \mathcal{P}_\phi(k_3) \\
 &\quad \times \int_{-1}^1 \frac{d\mu_{12}}{2} \int_{-1}^1 \frac{d\mu_{13}}{2} \int_0^{2\pi} \frac{d\varphi_{13}}{2\pi} W_R(k_{123}) \mathcal{M}(k_{123}) \\
 &\quad \times \left\{ P_\phi(k_{12}) \left[\frac{1}{P_\phi(k_1)} + \frac{1}{P_\phi(k_2)} \right] \left[1 + \frac{P_\phi(k_{123})}{P_\phi(k_3)} \right] \right. \\
 &\quad \left. + P_\phi(k_{23}) \left[\frac{1}{P_\phi(k_2)} + \frac{1}{P_\phi(k_3)} \right] \left[1 + \frac{P_\phi(k_{123})}{P_\phi(k_1)} \right] + P_\phi(k_{31}) \left[\frac{1}{P_\phi(k_3)} + \frac{1}{P_\phi(k_1)} \right] \left[1 + \frac{P_\phi(k_{123})}{P_\phi(k_2)} \right] \right\}. \tag{37}
 \end{aligned}$$

Here, we have fixed the three vectors, \mathbf{k}_1 , \mathbf{k}_2 and \mathbf{k}_3 that appear in the expression of the trispectrum, as shown in Fig. 1. Hence, using the angular variables, θ_{12} , θ_{13} and φ_{13} , we have

$$\begin{aligned}
 k_{12} &= \sqrt{k_1^2 + k_2^2 + 2k_1k_2\mu_{12}}, \\
 k_{23} &= \sqrt{k_2^2 + k_3^2 + 2k_2k_3 \left(\sqrt{(1-\mu_{12}^2)(1-\mu_{13}^2)} \cos \varphi_{13} + \mu_{12}\mu_{13} \right)}, \\
 k_{13} &= \sqrt{k_1^2 + k_3^2 + 2k_1k_3\mu_{13}}, \tag{38}
 \end{aligned}$$

and

$$k_{123} = \sqrt{k_1^2 + k_2^2 + k_3^2 + 2k_1k_2\mu_{12} + 2k_1k_3\mu_{13} + 2k_2k_3 \left(\sqrt{(1-\mu_{12}^2)(1-\mu_{13}^2)} \cos \varphi_{13} + \mu_{12}\mu_{13} \right)}, \tag{39}$$

where $\mu_{ij} \equiv \cos \theta_{ij}$. In order to calculate the skewness more easily, let us consider the squeezed limit in momentum space, e.g., $k_1 \ll k_2 \simeq k_3$. In this limit, the equation for the skewness (36) can be reduced to

$$\tilde{S}_3 \Big|_{k_1 \ll k_2 \simeq k_3} \simeq 2\sigma_R^2 \int \frac{dk_1}{k_1} W_R(k_1) \mathcal{M}(k_1) \mathcal{P}_\phi(k_1), \quad (40)$$

and by considering other limiting cases, i.e., $k_2 \rightarrow 0$ and $k_3 \rightarrow 0$, we obtain

$$\tilde{S}_3 \simeq 6\sigma_R^2 \int \frac{dk}{k} W_R(k) \mathcal{M}(k) \mathcal{P}_\phi(k). \quad (41)$$

Based on the above approximate expression, we find a simple formula:

$$\sigma_R S_3(R) = 4.3 \times 10^{-4} f_{\text{NL}} \times \sigma_R^{0.13} (10^{12} h^{-1} M_\odot < M < 2 \times 10^{15} h^{-1} M_\odot). \quad (42)$$

This result seems to be close to those given in Refs. (De Simone, Maggiore & Riotto 2010; Enqvist, Hotchkiss & Taanila 2010)². Hence, we adopt the above expression in the following discussion. In a similar way, from the expression of the kurtosis (37), we can easily find that the kurtosis induced from the non-linearity parameter τ_{NL} becomes largest in the limit of $k_i \rightarrow 0$ ($i = 1, 2, 3, 4$) or $k_{ij} \rightarrow 0$ ($i \neq j = 1, 2, 3, 4$) (local type). Then, we have an approximate expression

$$\tilde{S}_4^\tau(R) \simeq 8 \int \frac{dk}{k} W_R(k) \mathcal{M}(k) \mathcal{P}_\phi(k) \times \tilde{S}_3(R) + 12A_\phi \sigma_R^4. \quad (43)$$

On the other hand, in the squeezed limit $k_i \rightarrow 0$ ($i = 1, 2, 3, 4$), the kurtosis which is proportional to the non-linearity parameter g_{NL} can be also reduced to (Chongchitnan & Silk 2010a; Enqvist, Hotchkiss & Taanila 2010)

$$S_4^g \equiv \frac{54}{25} \frac{g_{\text{NL}}}{\sigma_R^6} \tilde{S}_4^g, \quad (44)$$

$$\tilde{S}_4^g \simeq 2 \int \frac{dk}{k} W_R(k) \mathcal{M}(k) \mathcal{P}_\phi(k) \times \tilde{S}_3(R).$$

From these approximate expressions, we respectively obtain simple formulae for the kurtosis in the form

$$\sigma_R^2 S_4^\tau(R) = 1.9 \times 10^{-7} \tau_{\text{NL}} \times \sigma_R^{0.25} (10^{12} h^{-1} M_\odot < M < 2 \times 10^{15} h^{-1} M_\odot),$$

$$\sigma_R^2 S_4^g(R) = 9.4 \times 10^{-8} g_{\text{NL}} \times \sigma_R^{0.27} (10^{12} h^{-1} M_\odot < M < 2 \times 10^{15} h^{-1} M_\odot). \quad (45)$$

The result for $S_4^g(R)$ also is close to that obtained in Ref. (Enqvist, Hotchkiss & Taanila 2010)³. Hence in the following discussion, we also adopt the above expressions for the kurtosis as well as that for the skewness.

3.2.2 Difference between the Gaussian and the non-Gaussian mass functions

Based on the above calculations for the variance, σ_R^2 , the skewness, S_3 , and also the kurtosis, S_4 , the mass function can now be calculated. In the following discussion, we take values of the non-linearity parameters as $f_{\text{NL}} = 100$, $\tau_{\text{NL}} = 10^6$ and $g_{\text{NL}} = 0$. This value of τ_{NL} may be inconsistent with the observational constraint obtained by Ref. (Smidt et al. 2010) as $-0.6 < \tau_{\text{NL}}/10^4 < 3.3$ at 95% confidence level. However, there might be a caveat since in Ref. (Fergusson, Regan & Shellard 2010), the authors have claimed that the approach in Smidt et al. does not directly subtract the effect of anisotropic noise and other systematic effects which are important in obtaining an accurate and optimized result. Nonetheless, in order to emphasize the differences between the Gaussian mass functions and the non-Gaussian mass functions with the non-zero f_{NL} and the non-zero τ_{NL} cases, we take the above values.

In Fig. 2, we show that the mass function in the mass range between $5.0 \times 10^{14} h^{-1} M_\odot$ and $2.0 \times 10^{15} h^{-1} M_\odot$ at the redshift $z = 0$. The red thin line shows the mass function with the Gaussian density fluctuations given by Eq. (32). The blue dashed and green thick lines show the non-Gaussian mass function given by Eq. (31) in the cases with $f_{\text{NL}} = 100$ and $\tau_{\text{NL}} = g_{\text{NL}} = 0$ and $\tau_{\text{NL}} = 10^6$ and $f_{\text{NL}} = g_{\text{NL}} = 0$, respectively. From this figure, it is rather difficult to see the differences between the Gaussian and the non-Gaussian mass functions. In Fig. 3 we show the ratios between the Gaussian and the non-Gaussian mass functions defined by Eq. (34). The red dashed line shows $\mathcal{R}_{\text{NG}}(M, 0)$ with $f_{\text{NL}} = 100$ and $\tau_{\text{NL}} = g_{\text{NL}} = 0$ and the blue solid line shows that with $f_{\text{NL}} = g_{\text{NL}} = 0$ and $\tau_{\text{NL}} = 10^6$. The magenta dotted line is for the case with $\tau_{\text{NL}} = g_{\text{NL}} = 0$ and $f_{\text{NL}} = 30$ which is corresponding to the mean value of the current WMAP data (Komatsu et al. 2011). The black dashed-dotted line is for the case with $f_{\text{NL}} = g_{\text{NL}} = 0$ and $\tau_{\text{NL}} = 10^4$ which is consistent with the maximum allowed value obtained by Ref. (Smidt et al. 2010). From this figure, we infer that for both types of primordial non-Gaussianity, i.e., positive skewness and kurtosis, the mass functions can be systematically enhanced for more massive objects, as compared with the Gaussian case. The enhancement of the mass functions depends on the values of τ_{NL} and g_{NL} . We find that for the cases with $f_{\text{NL}} = 30$ and $\tau_{\text{NL}} = 10^4$ \mathcal{R}_{NG} are respectively 1.06 and 1.01 for $M = 2 \times 10^{15} h^{-1} M_\odot$. Hence, in both cases the effects of the primordial non-Gaussianity on the mass functions seem to

² As mentioned in Ref. (Enqvist, Hotchkiss & Taanila 2010), this result is different from that in the published version of Ref. (Chongchitnan & Silk 2010a). However, the authors in Ref. (Chongchitnan & Silk 2010a) have corrected the result in the arXiv version and their new derivation is now close to our result (42).

³ In addition to the expression derived for the skewness, the result for kurtosis in Ref. (Chongchitnan & Silk 2010a) has been corrected in the arXiv version and this is also close to our result (45).

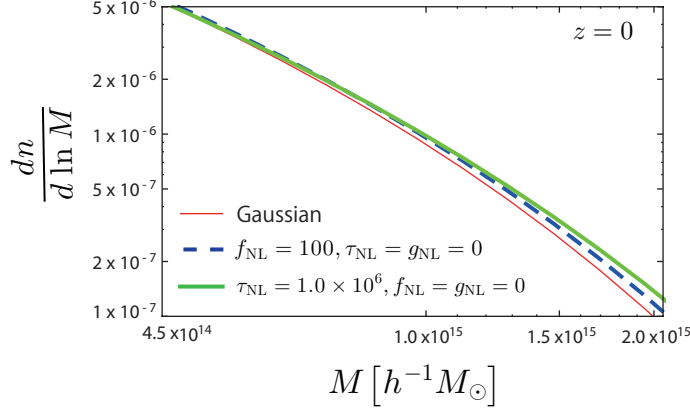


Figure 2. The mass function with the mass range between $4.5 \times 10^{14} h^{-1} M_{\odot}$ and $2.0 \times 10^{15} h^{-1} M_{\odot}$ at the redshift $z = 0$. The red thin line shows the mass function with the Gaussian density fluctuations given by Eq. (32). The blue dashed and green thick lines show the non-Gaussian mass function given by Eq. (31) in the case with $f_{\text{NL}} = 100$ and $\tau_{\text{NL}} = g_{\text{NL}} = 0$ and the case with $\tau_{\text{NL}} = 10^6$ and $f_{\text{NL}} = g_{\text{NL}} = 0$, respectively.

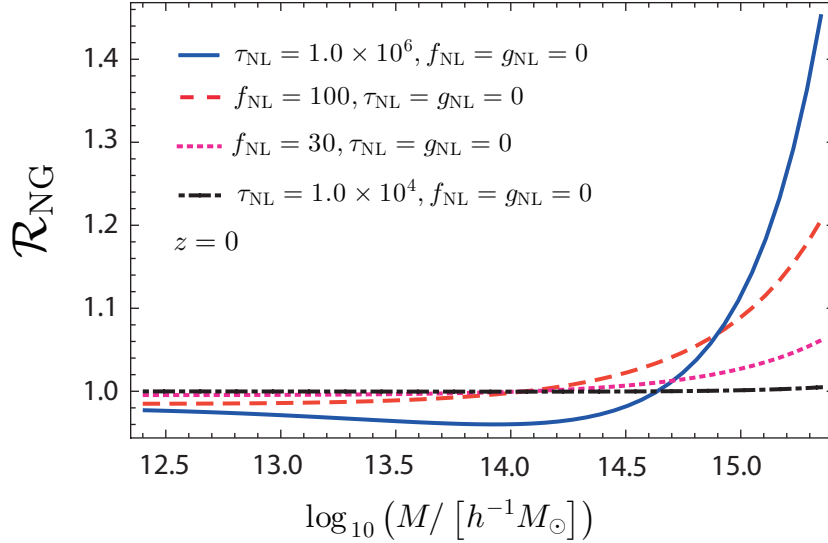


Figure 3. The ratio between the Gaussian and the non-Gaussian mass functions. The red dashed line shows $\mathcal{R}_{\text{NG}}(M, 0)$ with $f_{\text{NL}} = 100$ and $\tau_{\text{NL}} = g_{\text{NL}} = 0$ and the blue solid line shows that with $f_{\text{NL}} = g_{\text{NL}} = 0$ and $\tau_{\text{NL}} = 10^6$. The magenta dotted line is for the case with $\tau_{\text{NL}} = g_{\text{NL}} = 0$ and $f_{\text{NL}} = 30$ which is corresponding to the mean value of the current WMAP data (Komatsu et al. 2011). The black dashed-dotted line is for the case with $f_{\text{NL}} = g_{\text{NL}} = 0$ and $\tau_{\text{NL}} = 10^4$ which is consistent with the maximum allowed value obtained by Ref. (Smidt et al. 2010).

be too small to detect. We also find that the enhancement of the non-Gaussian mass function with the non-zero kurtosis type of primordial non-Gaussianity, i.e., non-zero τ_{NL} , depends more strongly on the mass of the collapsed objects than the case with the non-zero skewness type of primordial non-Gaussianity. This is because in the expression for the non-Gaussian mass function (31), the δ_c/σ_R -dependence of the term related with the kurtosis S_4 is stronger than that of the term related with the skewness S_3 , namely, S_4 -term $\propto (\delta_c/\sigma_R)^5$ and S_3 -term $\propto (\delta_c/\sigma_R)^4$. As the collapsed objects become more massive, the variance σ_R becomes smaller and hence δ_c/σ_R becomes larger. Thus, if we would detect the enhancement of the mass function for massive collapsed objects and find its scale-dependence, then we might distinguish the kurtosis type of primordial non-Gaussianity from the skewness type. In Fig. 4, we show the redshift dependence of the ratio between the non-Gaussian mass function and the Gaussian mass function as we change the value of τ_{NL} . Here we have fixed the mass of the halo as $M = 10^{14} h^{-1} M_{\odot}$. The solid line is for the case with $\tau_{\text{NL}} = 10^5$, the dashed line for 2.0×10^5 , dotted line for 5.0×10^5 and the dashed-dotted line for 10^6 . From this figure, we find that at higher redshift the enhancement of the mass function for massive collapsed objects increases. This is because the critical density $\delta_c(z) = \delta_c/D(z)$ becomes much larger at larger redshifts due to the smaller linear growth function $D(z)$. Hence, in order to observationally test the kurtosis type of primordial non-Gaussianity it will be useful to observe high-redshift rare objects.

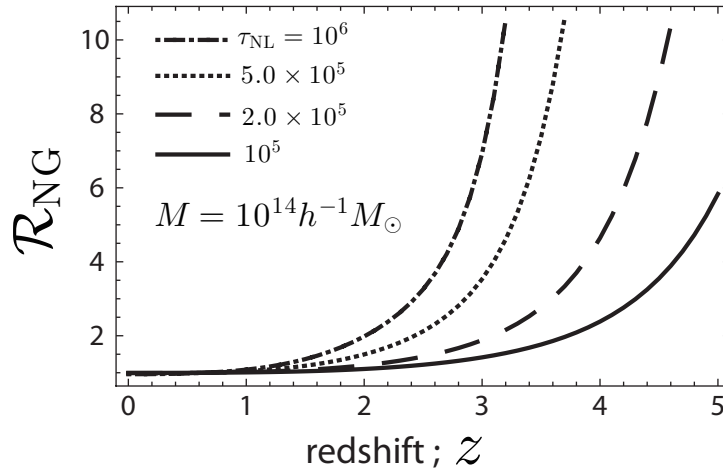


Figure 4. The ratio between the non-Gaussian mass function and the Gaussian mass function v.s. the redshift ($0 < z < 5$) with changing the value of τ_{NL} . Here we have fixed the mass of halo as $M = 10^{14} h^{-1} M_{\odot}$. The solid line is for the case with $\tau_{\text{NL}} = 10^5$, dashed line for 2.0×10^5 , dotted line for 5.0×10^5 and dot-dashed line for 10^6 .

4 APPLICATIONS

In this section, we consider applications of the mass function with both skewness and kurtosis types of primordial non-Gaussianity. Here, we also take values of the non-linearity parameters to be $f_{\text{NL}} = 100$, $\tau_{\text{NL}} = 10^6$ and $g_{\text{NL}} = 0$.

4.1 Early Star Formation

Let us first investigate the effect of primordial non-Gaussianity on the epoch of reionization. As is well-known, in order to understand the mechanism of reionization, it is important to estimate the number of photons from Population III stars. Following Refs. (Somerville & Livio 2003; Somerville, Bullock & Livio 2003; Sugiyama, Zaroubi & Silk 2004), the global star-formation-rate density denoted by $\dot{\rho}_*$ can be written as

$$\dot{\rho}_* = e_* \rho_b \frac{d}{dt} F_h(M_{\text{vir}} > M > M_{\text{crit}}, t). \quad (46)$$

Here, ρ_b is the background baryon number density and e_* denotes the star-formation efficiency usually taken to be 0.002 for $200 M_{\odot}$ Pop III stars and 0.001 for $100 M_{\odot}$. $F_h(M_{\text{vir}} > M > M_{\text{crit}}, t)$ represents the fraction of the total mass in collapsed objects (halos) with masses greater than the minimum collapse mass scale $M_{\text{crit}} = 10^6 h^{-1} M_{\odot}$ (Yoshida et al. 2003; Fuller & Couchman 2000) and lower than the virial mass $M_{\text{vir}} = M(T_{\text{vir}} = 10^4 \text{K})$.

The relation between the mass and the virial temperature is given by (Barkana & Loeb 2001; Yoshida et al. 2003)

$$T_{\text{vir}} = 4.7 \times 10^3 \left(\frac{\mu}{0.6} \right) \left(\frac{M}{10^8 h^{-1} M_{\odot}} \right)^{2/3} \left(\frac{\Omega_{m0} \Delta_c(z)}{0.24 \cdot 18\pi^2} \right)^{1/3} \left(\frac{1+z}{10} \right) \text{K} \quad (47)$$

where μ is the mean molecular weight, and $\Delta_c(z)$ is the final overdensity relative to the critical density, which is given by a fitting formula (Bryan & Norman 1998)

$$\Delta_c = 18\pi^2 + 82 (\Omega_m(z) - 1) - 39 (\Omega_m(z) - 1)^2, \quad (48)$$

where $\Omega_m(z)$ is the density parameter of matter at redshift z ;

$$\Omega_m(z) = \frac{\Omega_{m0}(1+z)^3}{\Omega_{m0}(1+z)^3 + \Omega_{\Lambda}}. \quad (49)$$

Assuming that the photon number production-rate per M_{\odot} from Pop. III stars is $N_{\gamma} = 1.6 \times 10^{48} s^{-1} M_{\odot}^{-1}$ and that the life time of Pop. III star is $\tau_{\text{III}} = 3.0 \times 10^6 \text{yr}$, we can obtain the total production rate of ionizing photons at time t as

$$\frac{dn_{\gamma}}{dt}(t) = e_* \rho_b N_{\gamma} (F_h(t) - F_h(t - \tau_{\text{III}})), \quad (50)$$

hence the cumulative number of photons per H atom is

$$\frac{n_{\gamma}}{n_H}(z) \simeq \mu m_p e_* N_{\gamma} F_h(M_{\text{vir}} > M > M_{\text{crit}}, z) \tau_{\text{III}}, \quad (51)$$

with the proton mass m_p and the hydrogen number density n_H . In the above expression, $F_h(M_{\text{vir}} > M > M_{\text{crit}}, z)$ is given by Press-

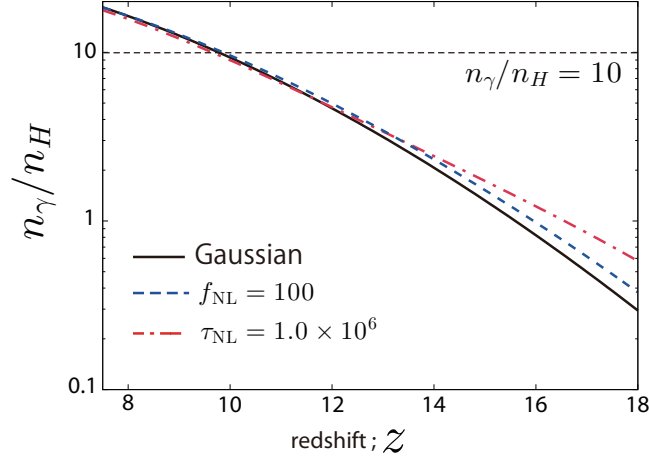


Figure 5. Cumulative photon number per H atom as a function of the redshift for $8 < z < 18$. The black solid line shows $n_\gamma/n_H(z)$ for the case with the Gaussian fluctuations. The blue dashed line is for the case with the non-Gaussian fluctuations; $f_{\text{NL}} = 100$ and $\tau_{\text{NL}} = g_{\text{NL}} = 0$. The red dot-dashed line is for the case with $\tau_{\text{NL}} = 1.0 \times 10^6$ and $f_{\text{NL}} = g_{\text{NL}} = 0$. The thin black dashed line corresponds to n_γ/n_H as a guide of the complete reionization.

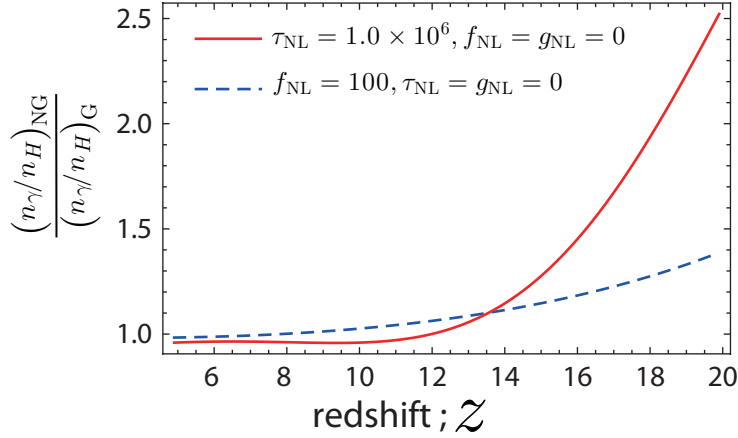


Figure 6. We plot the ratio between $n_\gamma(z)/n_H$ in the pure Gaussian primordial fluctuation case and that in the non-Gaussian case for $5 < z < 20$. The blue dashed line is for the case with $f_{\text{NL}} = 100$ and $\tau_{\text{NL}} = g_{\text{NL}} = 0$ and the red solid line for the case with $\tau_{\text{NL}} = 1.0 \times 10^6$ and $f_{\text{NL}} = g_{\text{NL}} = 0$.

Schechter theory as

$$F_h(M_{\text{vir}} > M > M_{\text{crit}}, z) = \frac{1}{\bar{\rho}} \int_{M_{\text{crit}}}^{M_{\text{vir}}} M \frac{dn}{dM}(M, z) dM. \quad (52)$$

Substituting our expression (31) for the non-Gaussian mass function into the above equation, we can estimate the effect of primordial non-Gaussianity on the number of photons emitted from Population III stars, which is one of the most important quantities during the epoch of reionization. In Fig. 5, we show the cumulative photon number per H atom given by Eq. (51) as a function of the redshift for $8 < z < 18$. The black solid line shows $n_\gamma/n_H(z)$ for the case with the Gaussian fluctuations, the blue dashed line is for the case with the non-Gaussian fluctuations; $f_{\text{NL}} = 100$ and $\tau_{\text{NL}} = g_{\text{NL}} = 0$ and the red dot-dashed line for the case with $\tau_{\text{NL}} = 1.0 \times 10^6$ and $f_{\text{NL}} = g_{\text{NL}} = 0$. The thin black dashed line corresponds to $n_\gamma/n_H = 10$ as a guide of the complete reionization on average. From this figure, we find that primordial non-Gaussianity seems not to affect the reionization history of the Universe on average which is characterized by the value of $n_\gamma/n_H = 10$. However, at higher redshift the effect of primordial non-Gaussianity seems to be significant on the cumulative photon number density. We evaluate this effect in Fig. 6, where we plot the ratio between $n_\gamma/n_H(z)$ in the pure Gaussian primordial fluctuation case and that in the non-Gaussian case. The blue dashed line is for the case with $f_{\text{NL}} = 100$ and $\tau_{\text{NL}} = g_{\text{NL}} = 0$ and the red solid line for the case with $\tau_{\text{NL}} = 1.0 \times 10^6$ and $f_{\text{NL}} = g_{\text{NL}} = 0$. From this figure, we find that compared to the Gaussian case the cumulative number of photons in the non-Gaussian case is larger at higher redshifts both in the non-zero S_3 and the non-zero S_4 cases. Moreover, as we have mentioned in the previous section the kurtosis type of primordial non-Gaussianity affects the enhancement of the photon number density more significantly at high redshift. That is, there seems to be the possibility of dramatically changing the history of the early stage of reionization due to the kurtosis type of primordial non-Gaussianity even for values in the range of the current limits obtained from CMB observations. Of course, the above rough estimate is not precise enough to enable us to estimate the exact cumulative number of the ionizing photons. However, we

consider here that, in view of the completely ad hoc nature of the amount of non-Gaussianity due to the absence of a compelling inflationary model, it suffices for us to focus on the deviation of the photon number based on the non-Gaussian mass function from that based on the Gaussian mass function.

4.2 High-Redshift Massive Clusters

Recently, the authors in Ref. (Jee et al. 2009; Rosati et al. 2009) have presented a weak lensing analysis of the galaxy cluster XMMU J2235.3-2557 which has a high redshift $z \approx 1.4$ and whose mass is $M_{324} = (6.4 \pm 1.2) \times 10^{14} M_\odot$ ⁴. In Λ CDM model the formation of such a massive cluster at this redshift would be a rare event (at least 3σ).

In Ref. (Cayon, Gordon & Silk 2010), the authors have considered the effects of primordial non-Gaussianity parametrized by the non-linearity parameter f_{NL} which they found to be $f_{\text{NL}} = 449 \pm 286$ at wave number of about 0.4Mpc^{-1} in order to explain the existence of such a massive cluster at high redshift. Considering scale-invariant f_{NL} , this result contradicts the current CMB observational constraint $f_{\text{NL}} < 100$. Therefore, the authors remarked that one would need to invoke scale-dependent f_{NL} . In Ref. (Enqvist, Hotchkiss & Taanila 2010), the authors have considered non-zero g_{NL} case and found that $g_{\text{NL}} = O(10^6)$ could explain the existence of high redshift massive clusters.

Here, instead of considering the scale-dependence of f_{NL} or g_{NL} , let us consider the effect of the kurtosis induced from the τ_{NL} -type primordial non-Gaussianity on the formation of massive clusters. Of course, for a more detailed analysis we need to calculate the probability of the massive clusters under the procedure done in Ref. (Cayon, Gordon & Silk 2010). However, in order to give a naive estimation of the value of τ_{NL} which can explain the existence of the massive cluster XMMU J2235.3-2557, we investigate the value of τ_{NL} which gives the same value as does the non-Gaussian mass function, namely, \mathcal{R}_{NG} defined as Eq. (34), including the effect of kurtosis S_4 on the corresponding scale at the corresponding redshift by including the effect of f_{NL} , i.e., skewness. Here, we adopt $M_{\text{XMMU}} = 6.4 \times 10^{14} M_\odot$ and $z_{\text{XMMU}} = 1.4$ as the mass and the redshift of the massive cluster XMMU J2235.3-255, respectively. For the value of f_{NL} , the best fit value derived in Ref. (Cayon, Gordon & Silk 2010) is adopted. For these parameters, we also find that this value can be realized in the case with $f_{\text{NL}} = g_{\text{NL}} = 0$ and $\tau_{\text{NL}} = 1.7 \times 10^6$. As we have mentioned in Sec. 3.2.2, this value may be ruled out by the result obtained by Ref. (Smidt et al. 2010). Hence, if we believe this constraint, we need to consider the possibility such as scale-dependent τ_{NL} .

4.3 Abundance of voids

As another example, we study the void abundance with primordial non-Gaussian corrections. In Ref. (Kamionkowski, Verde & Jimenez 2009), the authors showed that the void distribution function can be derived in the same way as the halo mass function using Press-Schechter theory. This is done by replacing the critical "overdensity" parameter, δ_c , with the negative "underdensity" parameter, δ_v . The precise value of δ_v depends on the definition of a void. For example, if the voids are regions having a density half of $\bar{\rho}$, then we can estimate the critical value of underdensity as $\delta_v \simeq -0.7$ (Kamionkowski, Verde & Jimenez 2009). There are also several numerical studies about the value of δ_v which suggest $\delta_v \approx -0.8$ (Shandarin et al. 2005; Park & Lee 2007; Colberg et al. 2008).

In any case, based on Press-Schechter theory, the abundance of voids which have radius between R and $R + dR$ is given by (Kamionkowski, Verde & Jimenez 2009)

$$\frac{dn^{\text{void}}(R)}{dR} dR = -dR \times \frac{6}{4\pi R^3} \frac{d}{dR} \int_{-\infty}^{\delta_v/\sigma_R} F(\nu) d\nu. \quad (53)$$

For pure Gaussian PDF, we have

$$\frac{dn_G^{\text{void}}(R)}{dR} = \sqrt{\frac{2}{\pi}} \frac{3}{4\pi R^4} \exp\left[-\frac{\delta_v^2}{2\sigma_R^2}\right] \frac{\delta_v}{\sigma_R} \frac{d \ln \sigma_R}{d \ln R}. \quad (54)$$

Up to the third order in terms of S_3 and S_4 , the void abundance with primordial non-Gaussian corrections is also given by

$$\begin{aligned} \frac{dn^{\text{void}}(R)}{dR} = & \sqrt{\frac{2}{\pi}} \frac{3}{4\pi R^4} \exp\left[-\frac{\delta_v^2}{2\sigma_R^2}\right] \left\{ \frac{d \ln \sigma_R}{d \ln R} \frac{\delta_v}{\sigma_R} \left[1 \right. \right. \\ & + \frac{S_3(R)\sigma_R}{6} H_3(\delta_v/\sigma_R) + \frac{1}{2} \left(\frac{S_3(R)\sigma_R}{6} \right)^2 H_6(\delta_v/\sigma_R) + \frac{1}{6} \left(\frac{S_3(R)\sigma_R}{6} \right)^3 H_9(\delta_v/\sigma_R) \\ & + \frac{S_4(R)\sigma_R^2}{24} H_4(\delta_v/\sigma_R) + \frac{1}{2} \left(\frac{S_4(R)\sigma_R^2}{24} \right)^2 H_8(\delta_v/\sigma_R) + \frac{1}{6} \left(\frac{S_4(R)\sigma_R^2}{24} \right)^3 H_{12}(\delta_v/\sigma_R) \left. \right] \\ & + \frac{d}{d \ln R} \left(\frac{S_3(R)\sigma_R}{6} \right) H_2(\delta_v/\sigma_R) + \frac{1}{2} \frac{d}{d \ln R} \left(\frac{S_3(R)\sigma_R}{6} \right)^2 H_5(\delta_v/\sigma_R) + \frac{1}{6} \frac{d}{d \ln R} \left(\frac{S_3(R)\sigma_R}{6} \right)^3 H_8(\delta_v/\sigma_R) \\ & + \frac{d}{d \ln R} \left(\frac{S_4(R)\sigma_R^2}{24} \right) H_3(\delta_v/\sigma_R) + \frac{1}{2} \frac{d}{d \ln R} \left(\frac{S_4(R)\sigma_R^2}{24} \right)^2 H_7(\delta_v/\sigma_R) + \frac{1}{6} \frac{d}{d \ln R} \left(\frac{S_4(R)\sigma_R^2}{24} \right)^3 H_{11}(\delta_v/\sigma_R) \left. \right\} \end{aligned} \quad (55)$$

⁴ The halo is defined as a spherical overdense region whose density is 324 times the mean matter density of the Universe.

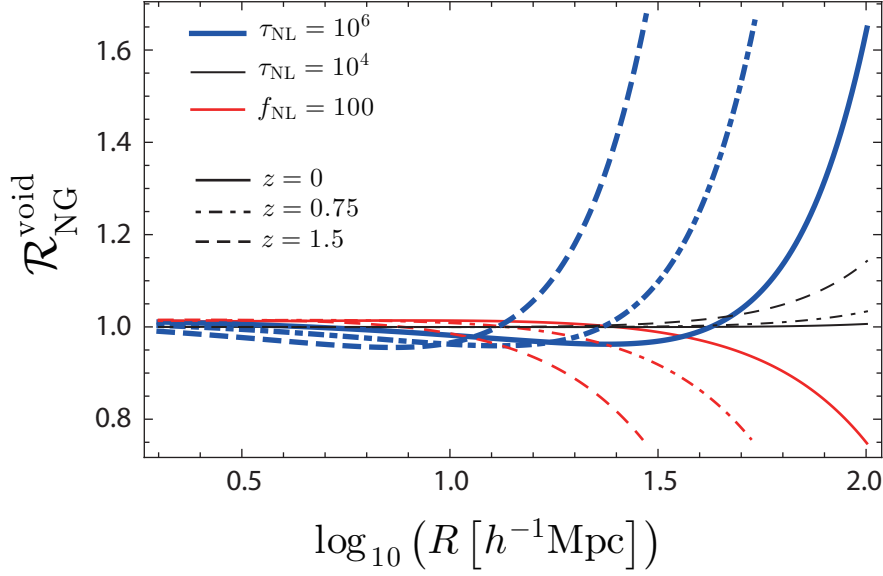


Figure 7. The ratio between the void abundance distribution function with non-zero primordial non-Gaussian correction and the Gaussian distribution function at redshifts $z = 0.0, 0.75, 1.5$ given by Eq. (56). The red lines are for the case with $f_{\text{NL}} = 100$ and $\tau_{\text{NL}} = g_{\text{NL}} = 0$, the blue thick lines for the case with $\tau_{\text{NL}} = 10^6$ and $f_{\text{NL}} = g_{\text{NL}} = 0$ and the black thin lines for the case with $\tau_{\text{NL}} = 10^4$ and $f_{\text{NL}} = g_{\text{NL}} = 0$. The solid lines are for the case with $z = 0.0$, the dot-dashed lines for the case with $z = 0.75$ and the dashed lines for the case with $z = 1.5$. Here we took $\delta_v = -0.7$.

Following the previous section, we define the ratio between the void abundance with the pure Gaussian PDF and that with the primordial non-Gaussian corrections as

$$\mathcal{R}_{\text{NG}}^{\text{void}} \equiv \frac{dn^{\text{void}}(R)/dR}{dn_{\text{G}}^{\text{void}}(R)/dR}. \quad (56)$$

In Fig. 7, we show $\mathcal{R}_{\text{NG}}^{\text{void}}$ for the cases with $f_{\text{NL}} = 100, \tau_{\text{NL}} = g_{\text{NL}} = 0$ (red lines), $\tau_{\text{NL}} = 10^6, f_{\text{NL}} = g_{\text{NL}} = 0$ (blue thick lines) and $\tau_{\text{NL}} = 10^4, f_{\text{NL}} = g_{\text{NL}} = 0$ (black thin lines). We adopt $\delta_v = -0.7$. We also show the ratio with changing the redshift; the solid lines for the case with $z = 0.0$, the dot-dashed lines for the case with $z = 0.75$ and the dashed lines for the case with $z = 1.5$. From this figure, we conclude that the non-Gaussian void abundance with non-zero τ_{NL} becomes larger than the Gaussian one on relatively larger scales whereas that with the non-zero f_{NL} becomes smaller. On the other hand, as seen in the previous section, the halo abundance becomes larger not only with non-zero τ_{NL} but also with non-zero f_{NL} in relatively more massive objects. Hence, from this discussion, we confirm that the non-Gaussian effects on both the halo and the void abundances allow us to distinguish the large kurtosis, i.e., large τ_{NL} , case from the large skewness, i.e., large f_{NL} case (Chongchitnan & Silk 2010a).

5 SUMMARY AND DISCUSSION

It has recently become clear that cosmological large-scale structure and CMB observations could provide stringent constraints on the PDF of primordial adiabatic curvature fluctuations. In particular, the high order moments of the PDF, such as its skewness and kurtosis, can give unique insights into the dynamics and conditions of the inflationary phase in the early Universe.

In this paper, we have investigated the effects of the τ_{NL} -type of primordial non-Gaussianity on the halo mass function. In particular, we have obtained a formula for the halo mass function with the non-Gaussian corrections coming from the kurtosis induced by the non-zero τ_{NL} . We find that the deviations of the non-Gaussian mass function from the Gaussian one become larger for larger mass objects ($M \gtrsim 10^{14} h^{-1} M_{\odot}$ for $z \sim 0$) as well as at higher redshifts ($z \gtrsim 1$ for $M \approx 10^{14} h^{-1} M_{\odot}$) in the case with $\tau_{\text{NL}} = O(10^6)$. Such features are quite similar to those obtained from skewness-driven non-Gaussian corrections that are induced by the f_{NL} -type of primordial non-Gaussianity.

As examples of applications of our formulae, we have considered the effects on early star formation, formation of the most massive objects at high redshift, and the abundance of voids.

For early star formation, we applied our formula for the non-Gaussian halo mass function in order to estimate of the redshift-dependence of the cumulative number of photons emitted from population III stars, a crucial quantity in considerations of the reionization history of the Universe. We found that primordial non-Gaussianity does not affect the reionization history of the Universe on the average, but at high redshift ($z \simeq 20$), namely the earliest stages of reionization, it is effective.

We have also obtained an estimate of the value of τ_{NL} needed to naturally explain the existence of the galaxy cluster XMMU J2235.3-2557, namely $\tau_{\text{NL}} = 1.7 \times 10^6$. Hence, in light of the result of Smidt et al., we might need to consider a possibility such as scale-dependent τ_{NL} in the case with non-zero f_{NL} . In Ref. (Hoyle, Jimenez & Verde 2010), the authors have investigated 15 high-mass and high-redshift galaxy clusters and found that such objects are extremely rare in the standard Λ CDM model with Gaussian primordial fluctuations. They derived a constraint on f_{NL} in order to explain the mere existence of these objects as $f_{\text{NL}} > 475$ at 95% confidence level, with the other cosmological parameters fixed to best fit values of WMAP data. In Ref. (Enqvist, Hotchkiss & Taanila 2010), the authors have extended the analysis of Ref. (Hoyle, Jimenez & Verde 2010) to the case with non-zero g_{NL} . It should clearly be of interest to derive a constraint on τ_{NL} for these observed high-mass and high-redshift galaxy clusters. We will address this in future work.

As mentioned in Refs. (Kamionkowski, Verde & Jimenez 2009; Chongchitnan & Silk 2010a), the non-Gaussian correction coming from skewness reduces the abundance of voids on large scales when the non-linearity parameter f_{NL} is positive in contrast to the fact that positive f_{NL} enhances the number of more massive halo objects. On the other hand, the non-Gaussian correction coming from kurtosis enhances not only the numbers of more massive halo objects but also the abundances of voids on large scales. Hence, if one could also measure the void abundance as well as the halo mass function more precisely, one could potentially distinguish between the f_{NL} and the τ_{NL} -types of primordial non-Gaussianity.

NOTE; During the time that we were preparing this manuscript, Ref. (LoVerde & Smith 2011) appeared on the arXiv. In Ref. (LoVerde & Smith 2011), they considered the same type of primordial non-Gaussianity as in our study and obtained a useful analytic formula for the halo mass function with the kurtosis type primordial non-Gaussianity using N-body simulations. We find that our formula (31) is in reasonably good agreement with their formula as far as the behavior of the halo mass function with the kurtosis type of primordial non-Gaussianity.

6 ACKNOWLEDGMENTS

S.Y. thanks Yoshitaka Takeuchi and Shogo Masaki, and J.S. thanks Laura Cayon, Sirichai Chongchitnan, and Christopher Gordon for valuable discussions. This work is supported by the Grant-in-Aid for Scientific research from the Ministry of Education, Science, Sports, and Culture, Japan, No. 22340056. The authors also acknowledge support from the Grant-in-Aid for Scientific Research on Priority Areas No. 467 “Probing the Dark Energy through an Extremely Wide and Deep Survey with Subaru Telescope” and the Grant-in-Aid for the Global COE Program “Quest for Fundamental Principles in the Universe: from Particles to the Solar System and the Cosmos” from MEXT, Japan. This work is also supported in part by World Premier International Research Center Initiative, MEXT, Japan.

REFERENCES

- Barkana R., Loeb A., 2001, *Phys. Rep.*, 349, 125
 Bartolo N., Komatsu E., Matarrese S., Riotto A., 2004 *Phys. Rep.*, 402, 103
 Bartolo N., Matarrese S. and Riotto A., 2010, *Advances in Astronomy*, 2010, 157079
 Bryan G. L., Norman M. L., 1998, *ApJ*, 495, 80
 Byrnes C. T., Choi K. Y., 2010, *Advances in Astronomy*, 2010, 724525
 Cayon L., Gordon C., Silk J., 2010, preprint (arXiv:1006.1950)
 Chongchitnan S., Silk J., 2010, *ApJ*, 724, 285
 Chongchitnan S., Silk J., 2011, *Phys. Rev. D*, 83, 083504
 Colberg J. M. et al., 2008, *MNRAS*, 387 933
 D’Amico G., Musso M., Norena J., Paranjape A., 2011, *J. Cosmology Astropart. Phys.*, 02, 01
 De Simone A., Maggiore M., Riotto A., 2010, preprint (arXiv:1007.1903)
 Desjacques V., Seljak U., 2010, *Phys. Rev. D*, 81, 023006
 Enqvist K., S. Sloth M., 2002, *Nucl. Phys. B*, 626, 395
 Enqvist K., Hotchkiss S., Taanila O., 2010, preprint (arXiv:1012.2732)
 Fergusson J. R., Regan D. M., Shellard E. P. S., 2010, preprint (arXiv:1012.6039).
 Fuller T. M., Couchman H. M. P., 2000, *ApJ*, 544, 6
 Gangui A., Lucchin F., Matarrese S., Mollerach S., 1994, *ApJ*, 430, 447
 Grossi M., Verde L., Carbone C., Dolag K., Branchini E., Iannuzzi F., Matarrese S., Moscardini L., 2009 *MNRAS*, 398, 321
 Hoyle B., Jimenez R., Verde L., 2011, *Phys. Rev. D*, 83, 103502
 Huang Q. G., 2009, *J. Cosmology Astropart. Phys.*, 06, 35
 Ichikawa K., Suyama T., Takahashi T., Yamaguchi M., 2008, *Phys. Rev. D*, 78, 023513
 Jee M. J. et al., 2009, *ApJ*, 704, 672
 Juszkiewicz R., Weinberg D. H., Amsterdamski P., Chodorowski M., Bouchet F., 1995, *ApJ*, 442, 39
 Kamionkowski M., Verde L., Jimenez R., 2009, *J. Cosmology Astropart. Phys.*, 01, 10
 Komatsu E., Spergel D. N., 2001, *Phys. Rev. D*, 63, 063002
 Komatsu E. et al. [WMAP Collaboration], 2011, *ApJ*, Suppl., 192, 18
 Komatsu E., 2010, *Classical and Quantum Gravity*, 27, 124010
 Langlois D., Vernizzi F., 2004, *Phys. Rev. D*, 70, 063522
 LoVerde M., Miller A., Shandera S., Verde L., 2008, *J. Cosmology Astropart. Phys.*, 04, 14

- LoVerde M., Smith K. M., 2011, preprint (arXiv:1102.1439)
 Lyth D. H., Wands D., 2002, Phys. Lett. B, 524, 5
 Matarrese S., Verde L., Jimenez R., 2000, ApJ, 541, 10
 Maggiore M., Riotto A., 2010, ApJ, 717, 526
 Maggiore M., Riotto A., 2010, MNRAS, 405, L1244
 Moroi T., Takahashi T., 2001, Phys. Lett. B, 522, 215 [Erratum-ibid. B, 539, 303]
 Park D., Lee J., 2007, Phys. Rev. Lett., 98, 081301
 Rosati P. et al., 2009, A & A, 508, 583
 Salopek D. S., Bond J. R., 1990, Phys. Rev. D, 42, 3936
 Shandarin S., Feldman H. A., Heitmann K., Habib S., 2006 MNRAS, 367, 1629
 Slosar A., Hirata C., Seljak U., Ho S., Padmanabhan N., 2008, J. Cosmology Astropart. Phys., 08, 31
 Smidt J., Amblard A., Byrnes C. T., Cooray A., Heavens A., Munshi D., 2010, Phys. Rev. D, 81, 123007 (2010)
 Smith K. M., LoVerde M., 2010, preprint (arXiv:1010.0055)
 Somerville R. S., Livio M., 2003, ApJ, 593, 611
 Somerville R. S., Bullock J. S., Livio M., 2003, ApJ, 593, 616
 Sugiyama N., Zaroubi S., Silk J., 2004, MNRAS, 354, 543
 Sugiyama N. S., Komatsu E., Futamase T., 2011, preprint (arXiv:1101.3636)
 Suyama T., Yamaguchi M., 2008, Phys. Rev. D, 77, 023505
 Suyama T., Takahashi T., Yamaguchi M., Yokoyama S., 2010, J. Cosmology Astropart. Phys. 12, 30
 Tseliakhovich D., Hirata C., Slosar A., 2010, Phys. Rev. D, 82, 043531
 Verde L., Wang L. M., Heavens A., Kamionkowski M., 2000, MNRAS, 313, L141
 Verde L., Jimenez R., Kamionkowski M., Matarrese S., 2001, MNRAS, 325, 412
 Verde L., 2010, Advances in Astronomy, 2010, 768675
 Wagner C., Verde L., Boubekur L., 2010, J. Cosmology Astropart. Phys. 10, 22
 Yoshida N., Abel T., Hernquist L., N. Sugiyama N., 2003, ApJ, 592, 645

APPENDIX A: MVJ EXPRESSION

In Ref. (Matarrese, Verde & Jimenez 2000), the authors have given a formula for the ratio between the non-Gaussian mass function and the Gaussian mass function as

$$\begin{aligned}
 R_{\text{NG}}^{\text{MVJ}}(M, z) &= \exp \left[\nu_c^3 \frac{S_3(R)\sigma_R}{6} + \nu_c^4 \frac{S_4(R)\sigma_R^2}{24} \right] \times \left[\delta_3 + \frac{\nu_c}{\delta_3} \left(-\frac{S_3(R)\sigma_R}{6} \right) + \left(\frac{d \ln \sigma_R}{dM} \right)^{-1} \frac{d}{dM} \left(\frac{S_3(R)\sigma_R}{6} \right) \right] \\
 &\quad \times \left[\delta_4 + \frac{\nu_c^2}{\delta_4} \left(-\frac{S_4(R)\sigma_R^2}{12} \right) + \left(\frac{d \ln \sigma_R}{dM} \right)^{-1} \frac{d}{dM} \left(\frac{S_4(R)\sigma_R^2}{24} \right) \right], \\
 \delta_3 &\equiv \left(1 - \nu_c \frac{S_3(R)\sigma_R}{3} \right)^{1/2}, \quad \delta_4 \equiv \left(1 - \nu_c^2 \frac{S_4(R)\sigma_R^2}{12} \right)^{1/2},
 \end{aligned} \tag{A1}$$

which was not derived based on the Edgeworth expansion as mentioned in section 3. In section 4, we have discussed some applications of the non-Gaussian halo mass function.

As for the discussion in subsection 4.1 about early star formation, the redshift-dependence of the critical value of the cumulative photon number per H atom ($n_\gamma/n_H = 10$) is not so sensitive to primordial non-Gaussianity. In order to estimate more precisely how n_γ/n_H at high redshift is enhanced due to primordial non-Gaussianity, we should check which formula better describes the effect of primordial non-Gaussianity on the halo mass function. This is a future issue. In subsection 4.3, we have discussed the void abundance and noted that the kurtosis type of primordial non-Gaussianity can enhance the abundance of the large voids as opposed to the skewness type of primordial non-Gaussianity. This is just qualitative discussion.

On the other hand, the discussion in subsection 4.2 is so quantitative and hence we have investigated the difference of the estimated value of τ_{NL} for the observation of XMMU J2235.3-2557 between the case with MVJ expression and that with Eq. (31) given in section 3. Our naive estimated value of τ_{NL} given in subsection 4.2 is $\tau_{\text{NL}} = 1.7 \times 10^6$. For the case by making use of MVJ expression, we obtained $\tau_{\text{NL}} = 1.1 \times 10^6$. These values seem to be same order and hence the result does not extremely change.